CHARM PRODUCTION IN DEEP INELASTIC LEPTON-HADRON SCATTERING*

W.L. VAN NEERVEN

Instituut-Lorentz, University of Leiden
POB 9506, 2300 RA Leiden, The Netherlands

(Received August 26, 1997)

A review is given of the QCD corrections to charm quark production in deep inelastic electron-proton scattering. An outline of the computation of the virtual photon-parton subprocesses, from which one obtains the heavy quark coefficient functions, is given. The dominant production mechanisms are discussed. Further we show that the asymptotic heavy quark coefficient functions, computed in the limit $Q^2 \gg m^2$, can be derived using the operator product expansion technique. Further we present the various schemes proposed in the literature to describe the charm component of the structure function and compare them with the most recent data from the experiments carried out at HERA.

PACS numbers: 13.10. +q

1. Introduction

The study of heavy quarks and their decay and production mechanisms provides us with important insights in the standard model of the electroweak and strong interactions. In this model the heavy flavours are given by the charm (c), bottom (b) and the top (t) quarks. Because of the confinement property in the theory of the strong interactions, given by quantum chromodynamics (QCD), these quarks can only be observed via the heavy baryons and mesons in which they are confined. Since mesons are more copiously produced than baryons we concentrate on the former particles. Here one can distinguish between the following types of mesons.

* Presented at the XXXVII Cracow School of Theoretical Physics, Zakopane, Poland, May 30–June 10, 1997.

1. **Open heavy quark mesons**

   In this case the heavy quark is accompanied by a lighter quark mostly represented by the up (u), down (d) and strange (s) quarks. Examples are:

   (a) open charm *e.g.* $D_u = \bar{u}c$, $D_d = \bar{d}c$, $D_s = \bar{s}c$.

   (b) open bottom *e.g.* $B_u = \bar{u}b$, $B_d = \bar{d}b$, $B_s = \bar{s}b$, $B_c = \bar{c}b$

   including their anti-mesons.

2. **Hidden heavy quark mesons**

   Here the heavy quark is always bound to its anti-quark. Examples are:

   (a) hidden charm *e.g.* $\mathcal{J}/\psi = \bar{c}c$

   (b) hidden bottom *e.g.* $\Upsilon = \bar{b}b$

   including the higher excitations.

In these lectures we limit ourselves to open heavy quark production. The mesons are observed via their electroweak decays. An example is the decay of the meson D_u given by $D_u \to K^- + \mu^+ + \nu_\mu$ which proceeds via the partonic reaction $c \to s + \mu^+ + \nu_\mu$ where μ^+, ν_μ emerge from the virtual W^+-boson which is exchanged between the quarks and the lepton pair.

There are numerous reasons why open heavy quark mesons are of interest. Here we will mention some of them (for a review see [1]).

(a) The observation of rare decays in particular those of the B-mesons. With rare we mean decays that are suppressed in the standard model.

(b) The measurement of the Cabibbo-Kobayashi-Maskawa matrix elements denoted by V_{ij} $(i, j = u, d \cdots t)$ via the production or decay of the heavy quark mesons. A classical example is the measurement of the quantity $V_{cs} = \cos\theta_c$ in the process $e + p \to \nu_e + D + X'$ ($'X'$ is any inclusive final state). For this reaction the dominant partonic subprocess is given by $e + s \to \nu_e + c$ which proceeds via the exchange of a W-boson.

(c) The study of $D\bar{D}$ and $B\bar{B}$-mixing in connection with CP- violation in the B-system.

(d) The study of production mechanisms of heavy quarks provides us with new tests of QCD. It also enables us to measure some of the parton densities (see below) in kinematical regions which are not accessible in other types of processes. An example is the gluon density which can be measured via charm production at the HERA-collider.

In these lectures we will only study those production mechanisms of heavy quarks where the methods of perturbative QCD can be used. Reactions where only nonperturbative methods can be applied like *e.g.*, diffraction will not be treated here.

In perturbative QCD physical quantities can be expanded in the strong coupling constant $\alpha_s(\mu^2)$, where the scale μ has to be large, provided we are dealing with so called hard processes. The latter are described by the parton model including higher order QCD corrections. The hard processes are characterized by the property that all kinematical invariants, on which the quantities depend, become asymptotic whereas their mutual ratios are fixed. These ratios should neither become zero nor infinite. In the case of heavy quark production the above condition implies that the heavy quark mass m should become asymptotic too. Unfortunately these types of processes cannot be completely described by perturbative methods. All cross sections also contain nonperturbative parts. The latter are represented by the parton densities and the fragmentation functions whose properties will be discussed below.

Let us first enumerate the various reactions, including the basic partonic subprocesses, in which the heavy mesons are produced in a semi-inclusive way.

1. **hadron-hadron collisions**

   Example: $P + \bar{P} \to B + \bar{B} +' X'$

   Lowest order partonic subprocesses: $g + g \to b + \bar{b}$, $q + \bar{q} \to b + \bar{b}$

2. **lepton-hadron collisions**

   Example: $e + P \to D + \bar{D} +' X'$

   Lowest order partonic subprocess: $\gamma^* + g \to c + \bar{c}$

3. **photon-hadron collisions**

   Example: $\gamma + P \to D + \bar{D} +' X'$

   Lowest order partonic subprocess: $\gamma + g \to c + \bar{c}$

4. **photon-photon collisions**

   Example: $\gamma + \gamma \to D + \bar{D} +' X'$

   Lowest order partonic subprocess: $\gamma + \gamma \to c + \bar{c}$

5. **electron-positron collisions**

   Example: $e^+ + e^- \to B + \bar{B} +' X'$

   Lowest order partonic subprocess: $e^+ + e^- \to b + \bar{b}$

Notice that in reaction 4 one or both photons can be virtual (indicated by $*$). In these lectures we only concentrate on reaction 2 where the charm (anti-) quark is produced in deep inelastic lepton-hadron scattering. We show this process in more detail in Fig. 1, where the momenta of the virtual photon and the proton are denoted by q and p respectively. Notice that q is spacelike (*i.e.* $q^2 = -Q^2 < 0$). Further we assume that Q^2 is small enough so that the neutral current process with the exchange of a Z-boson is suppressed. The process becomes deep inelastic when Q^2 and $p \cdot q$ are large whereas the scaling variable $x = Q^2/2p \cdot q$ is kept fixed (*i.e.* $0 < x < 1$ but $x \neq 0$ and $x \neq 1$). When these kinematical conditions are satisfied then according to the parton model the proton can be viewed as a collection of free quarks and gluons (called partons). Each of them can be involved in the hard scattering without being influenced by the other partons which are called spectators. The latter produce the hadronic final state $'X'$. Integration over the momenta and summation over the quantum numbers of the spectators provides us with the probability that the gluon in Fig. 1 emerges from the proton with the fraction z of the proton's momentum. This probability is given by the parton density indicated by $f_g^P(z)$. This function can only be computed using nonperturbative methods in QCD. Unfortunately these methods are not available yet so that one either has to resort to models for $f_g^P(z)$ or one has to obtain this density from the data. The same holds for the quark parton densities denoted by $f_q^P(z)$. The incoming gluon in Fig. 1 is involved in a hard scattering with the photon so that a charm anti-charm quark pair is produced in the final state. The charm

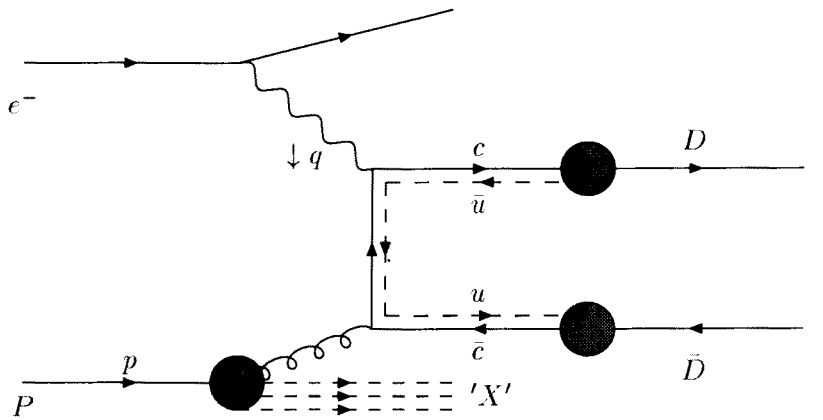

Fig. 1. Production of the mesons D and $\bar{D}$ in deep inelastic electron-proton scattering via the photon-gluon fusion mechanism.

and anti-charm quark pick up from the vacuum a light anti-quark and quark respectively. The fusion of the charm quark with the light anti-quark leads to the production of a D-meson. This process is described by the fragmentation function $\mathcal{D}_c^D(z)$ where z denotes the fraction of the momentum of the charm quark carried away by the D-meson. An analogous description holds for the production of the anti D-meson coming from the anti-charm and the light quark. The light (anti-) quarks, which are called spectators, have very low momenta so that they cannot change the magnitude as well as the direction of the three-momentum of the charm quark. Therefore the momentum of the charm quark can be reconstructed from the momentum of the D-meson. Like the parton densities the fragmentation functions can be only determined by using nonperturbative methods. However the latter are not at that stage that one can compute these functions. Therefore they can either be determined by models or they have to be extracted from the data. In spite of the poor knowledge about these functions one can assume that the parton densities $f_k^P(z)$ $(k = q, g)$ and the fragmentation functions $\mathcal{D}_k^a(z)$ $(a = D, B; k = c, b)$ are universal and process independent. The former only depend on the type of parton (q or g) and the type of hadron from which the parton emerges. The same holds for the fragmentation function which only depends on the heavy quark and the type of meson into which the former fragments. This universality remains unaltered even after QCD corrections to the hard processes have been included. It means that when these phenomenological functions are obtained from a certain process A one can use them as input for process B in order to make absolute predictions for the cross section of the latter reaction. This statement is only correct if the QCD corrections are carried out up to the same order in both processes.

2. Electroproduction of heavy quarks

Charm quark production in deep inelastic electron-proton scattering proceeds via the following reaction (see Fig. 2)

$$e^-(l_1) + P(p) \to e^-(l_2) + c(p_1)\,(\bar{c}(p_1)) +' X'. \tag{1}$$

Here $'X'$ denotes any inclusive hadronic state which means that we have summed over all quantum numbers and integrated over all momenta of the hadrons belonging to this state. Further we consider neutral current processes only so that the intermediate vector boson V either stands for the photon or for the Z-boson. The momentum transfer in the above process is spacelike so that we have

$$q^2 \equiv -Q^2 < 0 \qquad \text{with} \qquad q = l_1 - l_2\,. \tag{2}$$

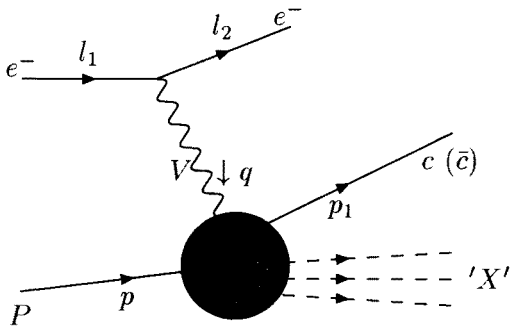

Fig. 2. Kinematics of charm production in deep inelastic electron-proton scattering

In the subsequent part of these lectures we will assume that $Q^2 \ll M_Z^2$ so that the above reaction is dominated by the one-photon exchange mechanism. The computation of the cross section of reaction (1) involves a five-dimensional integral. The kinematical integration variables are [2]

$$S = (p+q)^2 \quad , \quad \cos\Phi = \frac{(\vec{l}_1 \times \vec{l}_2).(\vec{p} \times \vec{p}_1)}{|\,\vec{l}_1 \times \vec{l}_2\,|\,.\,|\,\vec{p} \times \vec{p}_1)\,|}\,, \tag{3}$$

$$T_1 = T - m^2 = (p - p_1)^2 - m^2 \quad , \quad U_1 = U - m^2 = (q - p_1)^2 - m^2\,. \tag{4}$$

Further we define the scaling variables

$$x = \frac{Q^2}{2\,p \cdot q} \quad , \quad y = \frac{p \cdot q}{p \cdot l_1}\,. \tag{5}$$

Integration over Φ yields the following cross section

$$\frac{d^4\sigma(T_1, U_1, x, y)}{dx\,dy\,dT_1\,dU_1} = \frac{\alpha}{2\pi\,x\,y}\left[2(1-y)\frac{d^2\sigma_L(T_1, U_1, x)}{dT_1\,dU_1} + \{1 + (1-y)^2\}\frac{d^2\sigma_T(T_1, U_1, x)}{dT_1\,dU_1}\right], \tag{6}$$

where σ_L and σ_T stand for the longitudinal and transverse photon cross sections, respectively. In addition to the variables indicated above σ and σ_k $(k = T, L)$ also depend on Q^2 Eq. (2) and the heavy quark mass m. The factor in front of $d^2\sigma_T$ in Eq. (6) reflects the vector nature of the photon. From $d^2\sigma_k/dT_1 dU_1$ in Eq. (6) one can compute the double differential cross sections [3]

$$\frac{d^2\sigma_k}{dY\,d\,|\,\vec{p}_{1\perp}\,|} \quad , \quad \frac{d^2\sigma_k}{dX_f\,d\,|\,\vec{p}_{1\perp}\,|}\,. \tag{7}$$

The rapidity Y and the momentum fraction X_f are defined by

$$Y = \frac{1}{2}\ln\left(\frac{E_1 + \mid \vec{p}_{1l} \mid}{E_1 - \mid \vec{p}_{1l} \mid}\right) \quad , \quad X_f = \frac{\mid \vec{p}_{1l} \mid}{\mid \vec{p}_l \mid} . \tag{8}$$

In the above equations the longitudinal and the transverse momenta are indicated by the indices l and $\perp$ respectively. In the subsequent part of these lectures we are only interested in the integrated cross sections given by

$$\sigma_k(x, Q^2, m^2) = \int dT_1 \int dU_1 \frac{d^2\sigma_k(T_1, U_1, x, Q^2, m^2)}{dT_1\, dU_1} . \tag{9}$$

The total longitudinal and transverse cross sections are related to the corresponding deep inelastic structure functions F_k $(k = T, L)$ as follows

$$\begin{aligned} \sigma_L(x, Q^2, m^2) &= \frac{4\pi^2\alpha}{Q^2} F_L(x, Q^2, m^2) , \\ \sigma_T(x, Q^2, m^2) &= \frac{4\pi^2\alpha}{p \cdot q} F_1(x, Q^2, m^2) . \end{aligned} \tag{10}$$

Instead of F_1 the experimentalists measure the structure function

$$F_2(x, Q^2, m^2) = 2\, x\, F_1(x, Q^2, m^2) + F_L(x, Q^2, m^2) . \tag{11}$$

With the above definitions the deep inelastic scattering cross section can be written as

$$\frac{d^2\sigma}{dx\, dy} = \frac{2\pi\alpha^2}{Q^2} S_{eP}\Big[\{1 + (1-y)^2\} F_2(x, Q^2, m^2) - y^2 F_L(x, Q^2, m^2)\Big] . \tag{12}$$

Here $\sqrt{S_{eP}}$ denotes the centre of mass energy of incoming electron-proton system. When the charm component of the structure function is under study we will add an index c to the structure functions so F_k is replaced by $F_{k,c}$. Before we continue it is important to emphasize that perturbative QCD can only predict the Q^2-evolution of the structure functions but not their x-dependence. The latter is partially determined by the parton densities which, as we have mentioned before, are of a nonperturbative origin.

For charm production in perturbative QCD one can distinguish between two different production mechanisms. Let us denote the proton state in the Fock space by

$$\begin{aligned} \mid P\rangle \;=\; & a_1 \mid \mathrm{uud}\rangle + a_2 \mid \mathrm{u\bar{u}, uud}\rangle + a_3 \mid \mathrm{d\bar{d}, uud}\rangle + a_4 \mid \mathrm{s\bar{s}, uud}\rangle \\ & + \sum_{H=c}^{t} a_H \mid H\bar{H}, \mathrm{uud}\rangle . \end{aligned} \tag{13}$$

The two possible production mechanisms are:

A Intrinsic heavy quark production [4]

Here we have $a_H \neq 0$ for at least one H with $H = c, b, t$. In the case of intrinsic charm we have $a_c \neq 0$ and $a_b = 0$, $a_t = 0$. The main production mechanism is given by the flavour excitation process

$$\gamma^* + c \to c\,, \tag{14}$$

which is a zeroth order process in the strong coupling constant α_s.

B Extrinsic heavy quark production [5]

Here we have $a_H = 0$ for $H = c, b, t$. The dominant production mechanism is now given by the photon-gluon fusion process. On the Born level (first order in α_s) it is given by (see Fig. 3)

$$\gamma^* + g \to c + \bar{c}\,. \tag{15}$$

Fig. 3. Feynman diagrams for the lowest-order photon-gluon fusion process contributing to the coefficient functions $H_{i,g}^{(1)}$.

Notice that in the case of extrinsic charm production only light quarks (u,d,s) and the gluon can appear in the initial state of the partonic processes since the probability that a charm quark emerges from the proton is zero. In these lectures we will limit ourselves to extrinsic charm production because the recent experiments at HERA [6, 7] indicate that the data favour this production mechanism so that $f_c^P = 0$.

3. Exact heavy quark coefficient functions up to order α_s^2

The calculation of the partonic cross sections denoted by $\hat{\sigma}_{i,k}$ is straightforward (see [5]). After using the same relations as presented for the structure functions in Eq. (12) we obtain the heavy quark coefficient functions represented by $H_{i,k}$ $(i = 2, L; k = q, g)$. The lowest order contribution to the structure functions corresponding to the graphs in Fig. (3) can be written

as

$$F_{i,c}^{(1)}(x,Q^2,m^2) = e_c^2 \int_x^{z_{\max}} \frac{dz}{z} \hat{f}_g^{\mathrm{S}}(x/z) \hat{H}_{i,g}^{(1)}(z,Q^2,\hat{m}^2,\hat{\alpha}_s)$$
$$\equiv e_c^2 \, \hat{f}_g^{\mathrm{S}} \otimes \hat{H}_{i,g}^{(1)} , \tag{16}$$

with $z_{\max} = Q^2/(Q^2+4m^2)$ and e_c denotes the charge of the heavy quark (here $e_c = 2/3$). The quantities $\hat{m}$, $\hat{\alpha}_s$ and $\hat{f}_g$ stand for the bare mass, bare coupling constant and bare gluon density respectively. The meaning of the latter function will be discussed later. Further the order α_s^n contribution to the heavy quark coefficient function will be denoted by $H_{i,k}^{(n)}$. Finally the superscript on the gluon density indicates that we are dealing with a singlet (S) quantity with respect to the flavour symmetry transformations. Here the flavour symmetry group is given by $\mathrm{SU}(n_f)$. In the case of charm production we choose $n_f = 3$. The order α_s corrections to the photon-gluon

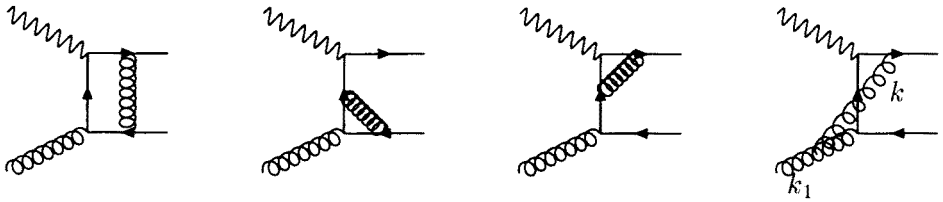

Fig. 4. Virtual gluon corrections to the proces $\gamma^* + g \to c + \bar{c}$ contributing to the coefficient functions $H_{i,g}^{(2)}$.

fusion process in Eq. (15) have been calculated in [2]. Some of the virtual contributions to the Born reaction are shown in Fig. 4. The corresponding Feynman integrals, denoted by $\mu^{4-N}(2\pi)^{-N} \int d^N k f(k,k_1)$, where k_1 is an external momentum, reveal ultraviolet (UV), infrared (IR) and collinear (C) divergences. They arise when the integration momentum k takes the values $k \to \infty$ (UV), $k = 0$ (IR) and $\vec{k} \| \vec{k}_1$ (C) respectively. The former two divergences are very well known in quantum field theory and we refer the reader to the textbooks. The collinear singularities originate from the propagator $1/(k-k_1)^2$ present in $f(k,k_1)$. It becomes singular when $k^2 = k_1^2 = 0$ so that $(k-k_1)^2 = -2 \mid \vec{k} \mid\mid \vec{k}_1 \mid (1-\cos\theta)$. The singularity then shows up at $\theta = 0$. The appearance of IR- and C-divergences is due to the fact that we neglect confinement effects in the initial and final state while doing perturbation theory. Here all external partons are put on-shell which is certainly not possible if we would have applied nonperturbative methods. In this case the partons are off-shell akin to the case when the

particles constitute a bound state. Fortunately there exist some theorems in quantum field theory which enable us to remove the divergences mentioned above. This will be discussed below. For the moment we have to find a way to define the Feynman integrals in which these divergences occur. For that purpose we choose the method of N-dimensional regularization which is the most suitable one since it preserves all Ward identities characteristic of gauge field theories. Using this method the divergences manifest themselves as pole terms of the type $1/\varepsilon^k$ with $\varepsilon = N - 4$.

Besides the virtual gluon graphs in Fig. 4 there are also contributions from the gluon bremsstrahlung diagrams in Fig. 5. This process is given by

$$\gamma^* + g \to c + \bar{c} + g\,. \tag{17}$$

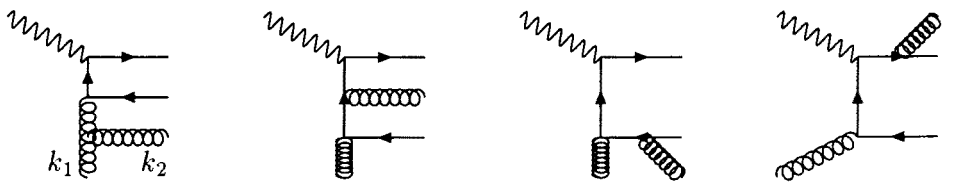

Fig. 5. The bremsstrahlungsprocess $\gamma^* + g \to c + \bar{c} + g$ contributing to the coefficient functions $H_{i,g}^{(2)}$.

Analogous to the one-loop Feynman integrals discussed above, IR and C divergences also show up in the phase space integrals corresponding to process (17). They arise when $k_2 \to 0$ (IR) and $\vec{k}_2 \| \vec{k}_1$ (C). The last condition originates from the propagator $f(k_1, k_2) \sim 1/(k_1 - k_2)^2$ appearing in the phase space integral $\mu^{4-N} \int d^{N-1}\vec{k}_2 (2E_2)^{-1} f(k_2, k_1)$. Addition of the virtual corrections to process (15) and the contributions from the bremsstrahlung reaction in (17)) leads to a cancellation of all IR singularities. This is called the Bloch-Nordsieck theorem [8]. Furthermore the Kinoshita-Lee-Nauenberg theorem [9] states that collinear divergences which can be attributed to the final state cancel too. This cancellation only happens when the final state is completely inclusive. Notice that up to the order in α_s discussed above final state collinear divergences are not present due to the heavy quark mass. The singularities which remain are of UV and initial state collinear origin. The former are removed by mass and coupling constant renormalization. Mass renormalization is performed by replacing the bare mass $\hat{m}$ in the lowest order coefficient function $H_{i,g}^{(1)}(z, Q^2, \hat{m}^2, \hat{\alpha}_s)$ via the substitution

$$\hat{m} = m\left[1 + \hat{a}_s\left(\frac{2}{\varepsilon}\delta_0 + d_1\right)\right] \quad \text{with} \quad \hat{a}_s \equiv \frac{\hat{\alpha}_s}{4\pi}\,. \tag{18}$$

After the substitution one has to make an expansion around $\hat{\alpha}_s$ which involves taking derivatives of $H_{i,g}$ with respect to m^2. Further d_1 is an arbitrary constant which is fixed by choosing the on-mass-shell scheme. After this renormalization the second order coefficient function takes the following form.

$$\hat{H}_{i,g}^{(2)} = \hat{a}_s \left[\left\{ \frac{1}{\varepsilon_C} + \frac{1}{2} \ln \left(\frac{m^2}{\mu^2} \right) \right\} P_{gg}^{(0)} \otimes H_{i,g}^{(1)} - \beta_0 \left\{ \frac{2}{\varepsilon_{UV}} + \ln \left(\frac{m^2}{\mu^2} \right) \right\} H_{i,g}^{(1)} \right] + H_{i,g}^{\text{finite},(2)} . \tag{19}$$

Here we have distinguished between the UV and the C-divergences which are indicated by $1/\varepsilon_{UV}$ and $1/\varepsilon_C$ respectively. Besides the higher order corrections to the photon-gluon fusion process there also exists another α_s^2 subprocess where the photon couples to the charm quark. It is given by the Bethe-Heitler reaction (see Fig. 6). Instead of a gluon we have now one of the light (anti-)quarks in the initial state and the reaction proceeds as follows

$$\gamma^* + q(\bar{q}) \to c + \bar{c} + q(\bar{q}) . \tag{20}$$

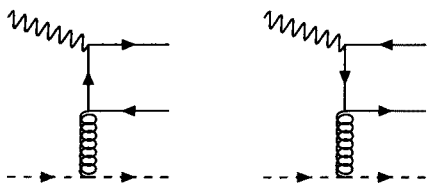

Fig. 6. The Bethe-Heitler process $\gamma^* + q \to c + \bar{c} + q$ contributing to the coefficient functions $H_{i,q}^{(2)}$.

In this process we only encounter collinear divergences and the bare heavy quark coefficient function reads

$$\hat{H}_{i,q}^{(2)} = \hat{a}_s \left\{ \frac{1}{\varepsilon_C} + \frac{1}{2} \ln \left(\frac{m^2}{\mu^2} \right) \right\} P_{gq}^{(0)} \otimes H_{i,g}^{(1)} + H_{i,q}^{\text{finite},(2)} . \tag{21}$$

Corrected up to order $\hat{\alpha}_s^2$ the structure function reads

$$F_{i,c} = e_c^2 \left[\hat{f}_g^{\text{S}} \otimes \left\{ \hat{H}_{i,g}^{(1)} + \hat{H}_{i,g}^{(2)} \right\} + \hat{f}_q^{\text{S}} \otimes \hat{H}_{i,q}^{(2)} + \cdots \right] . \tag{22}$$

Next we have to apply coupling constant renormalization in order to get rid of the remaining UV divergence. This is achieved by replacing

$$\hat{\alpha}_s = \alpha_s\left[1 + a_s\beta_0\left(\frac{2}{\varepsilon} + \ln\left(\frac{\mu_R^2}{\mu^2}\right) + b_1\right)\right] \tag{23}$$

in the coefficient function $\hat{H}_{i,g}^{(1)}(z, Q^2, m^2, \hat{\alpha}_s)$. In the above expression μ_R stands for the renormalization scale and $\alpha_s \equiv \alpha_s(\mu_R^2)$. Further β_0 denotes the lowest order coefficient appearing in the beta-function which will be defined below. The constant b_1 is scheme dependent. Here we will choose the $\overline{\text{MS}}$-scheme so that $b_1 = \gamma_E - \ln(4\pi)$ (γ_E is the Euler constant). Finally we have to perform mass factorization in order to get rid of the collinear divergence indicated by the pole term $1/\varepsilon_C$ in Eqs. (19), (21). This is achieved by replacing the bare $\hat{f}_k$ by the renormalized parton density f_k. In general one has

$$\hat{f}_l^{\text{S}} = f_k^{\text{S}}(\mu_F^2, \mu_R^2) \otimes \left[\delta_{kl} - a_s P_{kl}^{(0)}\left(\frac{1}{\varepsilon_C} + \frac{1}{2}\ln\left(\frac{\mu_F^2}{\mu^2}\right) + c_{kl}^{(1)}\right)\right], \tag{24}$$

where f_q^{S} denotes the singlet combination of the light flavour densities

$$f_q^{\text{S}} = \sum_{k=1}^{n_f}[f_k + f_{\bar{k}}]. \tag{25}$$

For $n_f = 3$, the index k runs over (u,d,s). Further μ_F stands for the factorization scale and $P_{kl}^{(0)}$ $(k, l = q, g)$ denote the lowest order DGLAP splitting functions. The constants $c_{kl}^{(1)}$ are scheme dependent. Here we will choose the $\overline{\text{MS}}$-scheme which implies that $c_{kl} = \gamma_E - \ln(4\pi)$. One can also perform mass factorization on the level of the heavy quark coefficient functions. In this case one gets the equation

$$\begin{aligned}&\hat{H}_{i,k}(Q^2, m^2, \alpha_s, \mu_R^2, \varepsilon_C, \mu^2)\\ &= \Gamma_{lk}(\alpha_s, \mu_R^2, \mu_F^2, \varepsilon_C, \mu^2) \otimes H_{i,l}(Q^2, m^2, \alpha_s, \mu_R^2, \mu_F^2),\end{aligned} \tag{26}$$

where Γ_{kl} denotes the transition function given by

$$\Gamma_{kl} = \delta_{kl} + a_s P_{kl}^{(0)}\left(\frac{1}{\varepsilon_C} + \frac{1}{2}\ln\left(\frac{\mu_F^2}{\mu^2}\right) + c_{kl}^{(1)}\right) + \cdots. \tag{27}$$

From Eq. (24) we infer that

$$f_k^{\text{S}}(\mu_R^2, \mu_F^2) = \Gamma_{kl}(\alpha_s, \mu_R^2, \mu_F^2, \varepsilon_C, \mu^2) \otimes \hat{f}_l^{\text{S}}. \tag{28}$$

In order to get finite coefficient functions up to order α_s^2 we need the following transition functions

$$\begin{aligned}
\Gamma_{qq} &= 1 + O(\alpha_s)\,, \\
\Gamma_{qg} &= O(\alpha_s)\,, \\
\Gamma_{gq} &= a_s P_{gq}^{(0)} \left(\frac{1}{\varepsilon_C} + \frac{1}{2} \ln \left(\frac{\mu_F^2}{\mu^2} \right) + c_{gq}^{(1)} \right) + \cdots\,, \\
\Gamma_{gg} &= 1 + a_s P_{gg}^{(0)} \left(\frac{1}{\varepsilon_C} + \frac{1}{2} \ln \left(\frac{\mu_F^2}{\mu^2} \right) + c_{gg}^{(1)} \right) + \cdots\,.
\end{aligned} \tag{29}$$

Notice that we have suppressed the z-dependence of the functions $P_{kl}^{(0)}$, $c_{kl}^{(1)}$ and $1 \equiv \delta(1-z)$. After renormalization and mass factorization the charm component of the structure function reads

$$F_{i,c} = e_c^2 [f_g \otimes \{H_{i,g}^{(1)} + H_{i,g}^{(2)}\} + f_q \otimes H_{i,q}^{(2)}]\,, \tag{30}$$

where $H_{i,g}^{(1)}$ is obtained from $\hat{H}_{i,g}^{(1)}$ by the substitution: $\hat{m} \to m$ and $\hat{\alpha}_s \to \alpha_s$. Further we introduce the shorthand notations

$$H_{i,g}^{(2)} = H_{i,g}^{\text{finite},(2)} + a_s \left(\frac{1}{2} \ln \left(\frac{m^2}{\mu_F^2} \right) P_{gg}^{(0)} \otimes H_{i,g}^{(1)} - \beta_0 H_{i,g}^{(1)} \ln \left(\frac{m^2}{\mu_R^2} \right) \right), \tag{31}$$

$$H_{i,q}^{(2)} = H_{i,q}^{\text{finite},(2)} + a_s \left(\frac{1}{2} \ln \left(\frac{m^2}{\mu_F^2} \right) P_{gq}^{(0)} \otimes H_{i,g}^{(1)} \right). \tag{32}$$

Besides the reactions discussed above where the photon interacts with the heavy quark the former can also couple to the light (anti-)quark. This happens for the first time in order α_s^2. In this order charm production proceeds via the Compton process (Fig. 7)) which is given by Eq. (20) where now the photon couples to the light (anti-)quark. The corresponding coefficient

Fig. 7. The Compton process $\gamma^* + q \to c + \bar{c} + q$ contributing to the coefficient functions $L_{i,q}^{(2)}$.

function is denoted by $L_{2,q}^{\rm NS}$ which in order α_s^2 is equal to $L_{2,q}^{\rm S}$. The structure function $F_{i,c}$ gets the contribution

$$F_{i,c} = \frac{1}{n_f} \sum_{k=1}^{n_f} e_k^2 \Big[f_q^{\rm S} \otimes L_{i,q}^{\rm S} + n_f f_k^{\rm NS} \otimes L_{i,q}^{\rm NS} \Big] . \tag{33}$$

The non-singlet combination of the quark densities is defined by

$$f_k^{\rm NS} = f_k + f_{\bar{k}} - \frac{1}{n_f} f_q^{\rm S} \qquad (k = u, d, s) . \tag{34}$$

Up to second order no collinear divergences appear in this type of processes. However in higher order they do appear. Moreover there are reactions with a gluon in the initial state leading to the heavy quark coefficient function $L_{i,g}^{\rm S}$. Together with $L_{i,q}^{\rm S}$ they satisfy the same mass factorization relations as presented for $H_{i,k}^{\rm S}$ in Eq. (26). For the non-singlet part a simpler relation holds (no mixing) which is given by

$$\hat{L}_{i,q}^{\rm NS} = \Gamma_{qq}^{\rm NS} L_{i,q}^{\rm NS} . \tag{35}$$

Likewise for the non-singlet parton density we have

$$f_k^{\rm NS} = \Gamma_{qq}^{\rm NS} \hat{f}_k^{\rm NS} . \tag{36}$$

The reason that the transition functions Γ_{kl} are the same for $H_{i,k}$ and $L_{i,k}$ follows from the universality of collinear divergences. It means that the latter are process independent. The same residues, represented by the DGLAP functions P_{kl}, are also found while calculating corrections to other hard processes differing from heavy flavour production. One of the most important consequences is that the finite parton densities also become universal after mass factorization so that one can use them as input for other processes to yield absolute predictions. Collecting all contributions the charm component of the deep inelastic structure function for the proton reads

$$\begin{aligned} F_{i,c}(n_f, Q^2, m^2) = \frac{1}{n_f} \sum_{k=1}^{n_f} e_k^2 \Big[& f_q^{\rm S}(n_f, \mu^2) \otimes L_{i,q}^{\rm S}(n_f, Q^2, m^2, \mu^2) \\ & + f_g^{\rm S}(n_f, \mu^2) \otimes L_{i,g}^{\rm S}(n_f, Q^2, m^2, \mu^2) \\ & + n_f f_k^{\rm NS}(n_f, \mu^2) \otimes L_{i,q}^{\rm NS}(n_f, Q^2, m^2, \mu^2) \Big] \\ & + e_c^2 \Big[f_q^{\rm S}(n_f, \mu^2) \otimes H_{i,q}^{\rm PS}(n_f, Q^2, m^2, \mu^2) \\ & + f_g^{\rm S}(n_f, \mu^2) \otimes H_{i,g}^{\rm S}(n_f, Q^2, m^2, \mu^2) \Big] , \end{aligned} \tag{37}$$

where now all quantities are finite. Notice that contrary to $L_{i,k}$ the functions $H_{i,k}$ are purely singlet (PS) only. This automatically holds for $H_{i,g}$. In the case of $k = q$ we have added the superscript PS because $H_{i,k}^{\rm NS} = 0$ (no intrinsic charm !!!). As we have shown above the coefficient functions and the parton densities depend on two different scales μ_R and μ_F. In order to simplify the renormalization group equations (RGE's) below we will set them equal *i.e.* $\mu_R = \mu_F = \mu$. Let us first define the total derivative with respect to μ.

$$D \equiv \mu \frac{d}{d\mu} = \mu \frac{\partial}{\partial \mu} + \beta(\alpha_s) \frac{\partial}{\partial \alpha_s}, \tag{38}$$

where $\beta(\alpha_s)$ denotes the beta-function which can be written as a series expansion in the strong coupling constant

$$\beta(\alpha_s) = -2\beta_0 \alpha_s^2 - 2\beta_1 \alpha_s^3 + \cdots . \tag{39}$$

One can show that the parton densities satisfy the following RGE's

$$D f_q^{\rm NS} = P_{qq}^{\rm NS} \otimes f_q^{\rm NS} \quad , \quad D f_k^{\rm S} = P_{kl}^{\rm S} \otimes f_l^{\rm S} . \tag{40}$$

The heavy quark coefficient functions satisfy the RGE's

$$\begin{aligned} D L_{i,q}^{\rm NS} &= -P_{qq}^{\rm NS} \otimes L_{i,q}^{\rm NS} \quad D L_{i,k}^{\rm S} = -P_{lk}^{\rm S} \otimes L_{i,l}^{\rm S} \\ D H_{i,k}^{\rm S} &= -P_{lk}^{\rm S} \otimes H_{i,l}^{\rm S} . \end{aligned} \tag{41}$$

The DGLAP splitting functions can be expanded in the coupling constant

$$P_{kl} = a_s P_{kl}^{(0)} + a_s^2 P_{kl}^{(1)} + \cdots . \tag{42}$$

Using the above equations one can now show that $F_{i,c}$ is a renormalization group invariant *i.e.* $D\, F_{i,c} = 0$. It means that it is a physical quantity which is independent of the scale μ and the chosen scheme. (Notice that in these lectures we have adopted the $\overline{\rm MS}$-scheme for the renormalization of the coupling constant and for mass factorization).

The order α_s^2 contributions to the heavy quark coefficient functions $H_{i,k}$ and $L_{i,k}$ have been computed in [2]. The expressions are so complicated that it is impossible to give analytic results. They are buried in long programs containing the numerical computation of two dimensional integrals. In order to make these coefficient functions more amenable for phenomenological applications they are tabulated [11] in the form of a two dimensional array in the variables

$$\eta = \frac{1-z}{4z}\xi - 1 \quad , \quad \xi = \frac{Q^2}{m^2} . \tag{43}$$

The first variable is chosen in such a way that the threshold region $\eta = (s-4m^2)(4m^2)^{-1} \sim 0$ is exposed in a clearer way. Notice that this region dominates the integrand of the structure function (see [12])

$$F_{i,c}(x,Q^2,m^2) \sim \int_x^{z_{\max}} \frac{dz}{z} f_k(x/z) H_{i,k}(z,Q^2,m^2)\,. \tag{44}$$

In Figs. 8, 9, 10 we have plotted the coefficient functions $H_{2,g}$, $H_{2,q}$ and $L_{2,q}$ respectively. Here we have chosen $m = m_c = 1.5$ GeV/c. From these plots we infer that $H_{2,g}$ is much larger than the two other heavy quark coefficient functions so that the photon-gluon fusion process constitutes the bulk of the radiative corrections. Since this process only depends on the gluon density $f_g^S(z,\mu^2)$ charm electroproduction yields a measurement of the latter density, in particular at small z. The coefficient functions reveal large corrections which occur in two regions given by

1 Threshold regime: $s \sim 4m^2$ or $z \sim z_{\max} = Q^2/(Q^2+4m^2)$

Here we have two types of large corrections. The first one is due to soft gluon bremsstrahlung. As we have discussed before the real gluon and the virtual gluon corrections show IR divergences when $k_2 \to 0$. In the real gluon case we have a phase space factor and the corresponding coefficient function behaves like

$$H_{i,g}^{(2),\mathrm{REAL}} \sim \frac{1}{\varepsilon_{\mathrm{IR}}}\left(\frac{s-4m^2}{4m^2}\right)^{\varepsilon_{\mathrm{IR}}/2} H_{i,g}^{(1)}\,. \tag{45}$$

On the other hand the virtual contribution equals

$$H_{i,g}^{(2),\mathrm{VIRT}} \sim -\frac{1}{\varepsilon_{\mathrm{IR}}} H_{i,g}^{(1)}\,. \tag{46}$$

Addition of the two expressions above leaves the finite result

$$H_{i,g}^{(2)} \sim \ln\left(\frac{s-4m^2}{4m^2}\right)\sigma_{i,g}^{(1)}\,, \tag{47}$$

which however blows up when $s \to 4m^2$. The above behaviour is typical for QED. In QCD we have a C-divergence in addition to the IR divergence. Hence after having removed the IR and C-singularities the power of the logarithms will be doubled. The final result in QCD shows the following behaviour

$$H_{i,g}^{(n)} \sim \alpha_s^n \ln^{2(n-1)}\left(\frac{s-4m^2}{4m^2}\right) H_{i,g}^{(1)}\,. \tag{48}$$

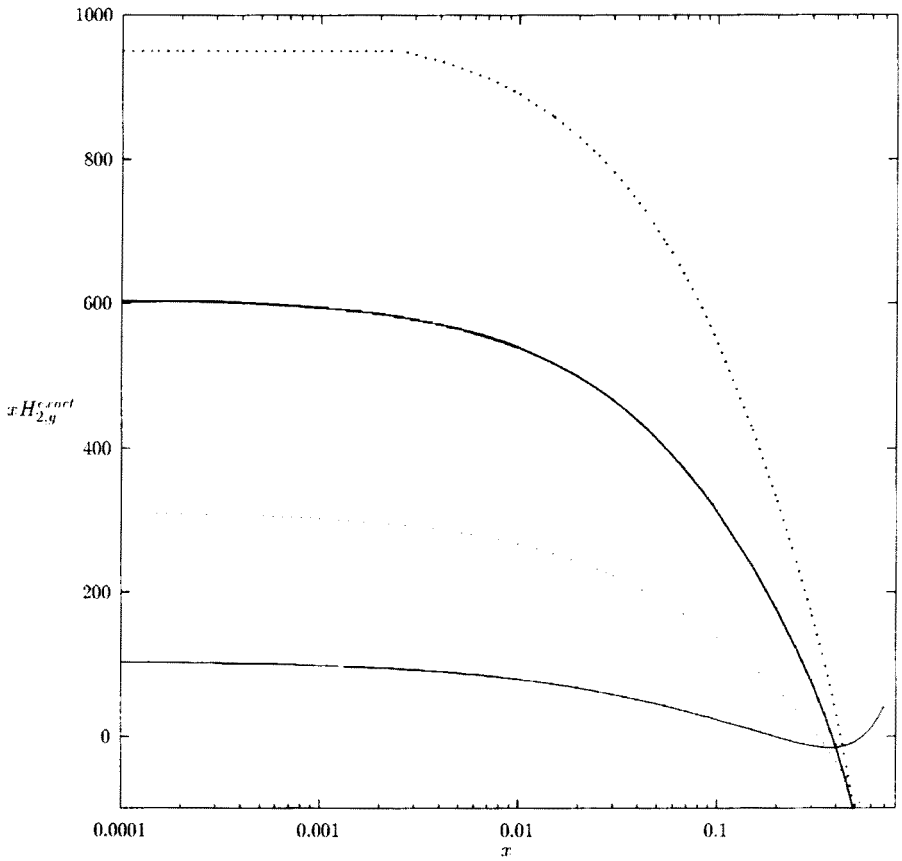

Fig. 8. The function $H_{2,g}(x, Q^2, m_c^2)$ for $Q^2 = 10$ (lower solid line), $Q^2 = 100$ (lower dotted line), $Q^2 = 10^3$ (upper solid line), $Q^2 = 10^4$ (upper dotted line). All units are in $(\mathrm{GeV}/c)^2$.

The above logarithms can be summed in all orders of perturbation theory by exponentiating them (see [13]). The effect of these logarithms is shown in Fig. 8 where we plotted $H_{2,g}^{(2)}$. In the threshold region where x is large and Q^2 is small one observes a rise in the coefficient function. Another large correction near threshold can be traced back to the Coulomb singularity appearing in the virtual contribution in

Fig. 12. One obtains the following expression

$$| M_g^{(2),\mathrm{VIRT}} |^2 \sim \frac{\pi^2}{\sqrt{(s-4m^2)}} \quad \rightarrow \quad H_{i,g}^{(2),\mathrm{VIRT}} \sim \frac{\pi^2}{m^2}. \tag{49}$$

This singularity is enhanced by multiple gluon exchanges between the heavy quark lines. It arises because we apply perturbation theory. The correct way to deal with these exchanges is to apply nonperturbative methods. In this case the nonperturbative result shows a singularity at $\alpha_s = 0$ which implies that one cannot make an expansion around this point. In practice the effect of the Coulomb singularity is so small that one can hardly see it in the heavy quark coefficient functions.

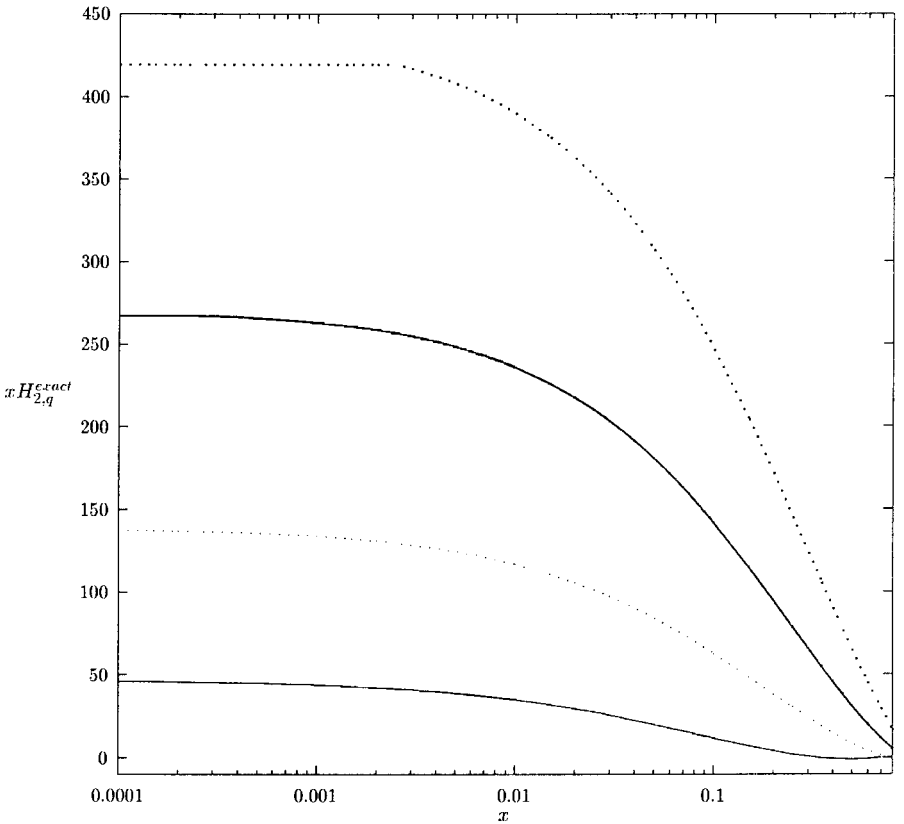

Fig. 9. Same as Fig. 8 for $H_{2,q}(x, Q^2, m_c^2)$.

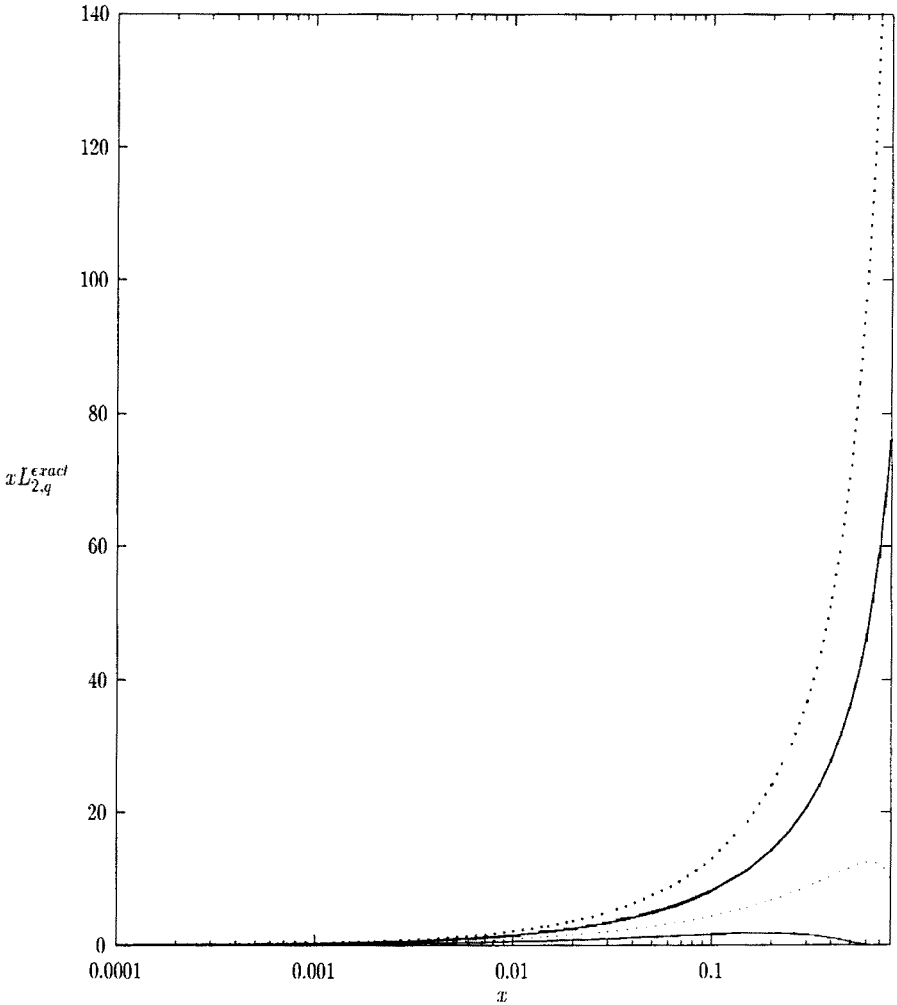

Fig. 10. Same as Fig. 8 for $L_{2,q}(x, Q^2, m_c^2)$.

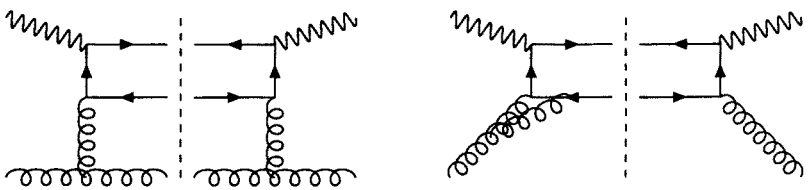

Fig. 11. Soft gluon contributions to the coefficient functions $H_{i,g}^{(2)}$.

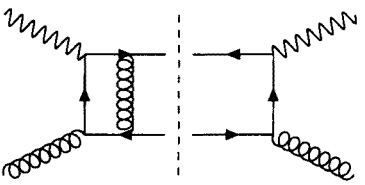

Fig. 12. The Coulomb singularity appearing in the box graph of the process $\gamma^* + g \to c + \bar{c}$.

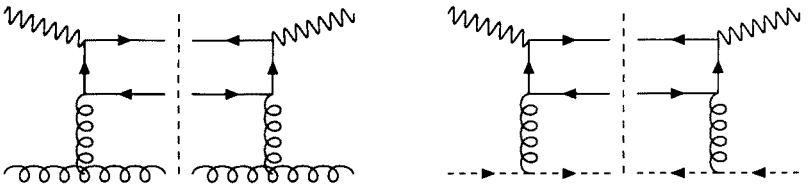

Fig. 13. Soft gluon exchanges in the t-channel of the processes: $\gamma^* + g \to c + \bar{c} + g$ and $\gamma^* + q \to c + \bar{c} + q$.

2 Asymptotic regime: $s \gg m^2$ or $z \to 0$.

The large corrections in this region are due to the exchange of multiple soft gluons in the t-channel. The corresponding coefficient functions have the form

$$H_{i,k}^{(n)}(z, Q^2, m^2) \underset{z \to 0}{\sim} \frac{1}{z} \ln^{n-2}(z) h(Q^2, m^2) \quad \text{for } n \geq 2; \quad k = q, g\,. \tag{50}$$

For $n = 2$ see Fig. 13. Like in the previous cases these large corrections can be resummed (see [14]). The soft gluon exchange mechanism has a huge effect on the heavy quark coefficient functions. It is responsible for the large plateau in the small x region of the functions $H_{2,g}^{(2)}$ (Fig. 8) and $H_{2,q}^{(2)}$ (Fig. 9). This plateau rises as Q^2 increases. However it turns out that this production mechanism is not so important for the behaviour of $F_{i,c}$ in Eq. (44) at small x since the main contribution to the integral comes from large z rather than small z.

4. Asymptotic heavy quark coefficient functions

As we mentioned in the previous section it is very hard to get analytical expressions for the second order heavy quark coefficient functions except for $L_{i,q}$ $(i = 2, L)$ which are published in [15]. However when $Q^2 \gg m^2$ it is possible to obtain analytical expressions. This is very useful because the latter serve as a check on the exact calculations carried out in [2, 11]. Furthermore it turns out that for charm production the asymptotic heavy quark coefficient functions give an equally good description as the exact ones when $Q^2 > 20\,(\mathrm{GeV}/c)^2$ and $x < 0.01$. Finally the asymptotic expressions can be also used for the charm component of the structure function (Eq. (37)) in the so called variable flavour number scheme (VFNS) discussed in the next section. In order to compute the asymptotic heavy quark coefficient functions one can proceed in two ways.

1 Standard method

In this case one evaluates all Feynman and phase space integrals for $Q^2 \gg m^2$. This method is still elaborate and one has to be careful with terms in these integrals which are proportional to $(m^2)^j$ because they survive in the limit indicated above.

2 Techniques of asymptotic expansions

Here we can use the operator product expansion (OPE) which is very elegant. As we will explain by presenting some examples one can compute the asymptotic expressions for $H_{i,k}$ and $L_{i,k}$ provided we know the massless parton coefficient functions denoted by $\mathcal{C}_{i,k}$ and the heavy quark operator matrix elements (OME's) given by A_{ck} and $A_{kl,c}$. $(k, l = q, g)$. Fortunately the functions $\mathcal{C}_{i,k}$ are already known up to order α_s^2 for some time [16]. Recently the OME's have also been computed up the same order (see [15, 17]) so that one can obtain the heavy quark coefficient functions without doing too much work.

Adopting the second method in the subsequent part of this section it is very easy to show that one obtains the following result in lowest order

$$H_{2,g}^{\mathrm{ASYMP},(1)}(z, Q^2, m^2) = a_s\left[P_{qg}^{(0)}(z)\ln\left(\frac{Q^2}{m^2}\right) + h_{2,g}^{(1)}(z)\right]. \tag{51}$$

The above equation can be easily inferred from the literature [5, 2] by taking the limit $Q^2 \gg m^2$ of the exact formula. The latter can be also obtained in the limit $m \to 0$. In this case the charm mass acts as a regulator for the C-divergence which is indicated by its residue represented by the DGLAP splitting function P_{qg} [10]. Because of the analogy between $\ln m^2$ and the

pole term $1/\varepsilon_C$ which represents the collinear divergence in the case of massless partons treated in the last section we can now apply mass factorization to remove them from the asymptotic heavy quark coefficient functions. In lowest order this is very simple and we obtain

$$H_{2,g}^{\mathrm{ASYMP},(1)}(z,Q^2,m^2) = C_{2,g}^{(1)}\left(z,\frac{Q^2}{\mu^2}\right) + A_{cg}^{(1)}\left(z,\frac{\mu^2}{m^2}\right), \tag{52}$$

with

$$C_{2,g}^{(1)}\left(z,\frac{Q^2}{\mu^2}\right) = a_s\left[P_{qg}^{(0)}(z)\ln\left(\frac{Q^2}{\mu^2}\right) + c_{2,g}^{(1)}(z)\right], \tag{53}$$

and

$$A_{cg}^{(1)}\left(z,\frac{\mu^2}{m^2}\right) = a_s\left[P_{qg}^{(0)}(z)\ln\left(\frac{\mu^2}{m^2}\right) + a_{cg}^{(1)}(z)\right]. \tag{54}$$

Here we want to stress the analogy between the quantities treated in the previous and the present section. They are

Section 3	Section 4
$\hat{H}_{i,k}(z,Q^2,m^2,\varepsilon_C)$	$H_{i,k}^{\mathrm{ASYMP}}(z,Q^2,m^2)$
$H_{i,k}(z,Q^2,m^2,\mu^2)$	$C_{i,k}\left(z,\frac{Q^2}{\mu^2}\right)$
$\Gamma_{kl}(z,\mu^2,\varepsilon_C)$	$A_{ck}\left(z,\frac{\mu^2}{m^2}\right)$.

(55)

In particular we want to emphasize the similar role played by the transition functions Γ_{kl} and the OME's A_{ck}. Both of them absorb the collinear divergences from the original quantities. We will now show that in lowest order the quantity $A_{cg}^{(1)}$ really stands for the heavy quark OME.

Squaring the amplitude corresponding to the Feynman graphs in Fig. 1 and integrating over the final particle phase space one can apply the optical theorem which states that

$$H_{i,k}(s,Q^2,m^2) = \mathrm{Im}\, T_{i,k}(s,Q^2,m^2), \tag{56}$$

where $z = s/(s+Q^2)$. Here $T_{i,k}$ stands for the forward Compton scattering amplitude (Fig. 14) and the discontinuity denoted by Im is taken over the

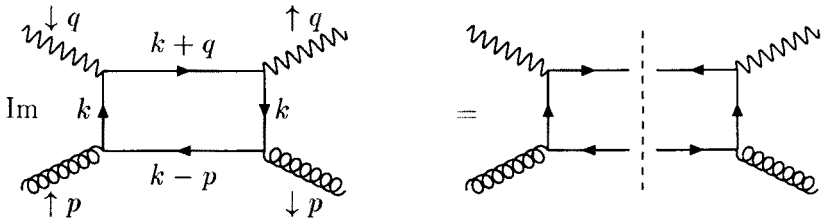

Fig. 14. Forward Compton scattering : $\gamma^* + g \to \gamma^* + g$ and the optical theorem

s-channel. If we define $\nu = p \cdot q = (s - m^2 + Q^2)/2$ one can write an unsubtracted dispersion relation which can be expressed as follows

$$\begin{aligned} T_{i,k}(\nu, Q^2, m^2) &= \frac{1}{\pi} \int\limits_{Q^2/2}^{\infty} d\nu' \frac{H_{i,k}(\nu', Q^2, m^2)}{\nu' - \nu} \\ &= \frac{z}{\pi} \int\limits_0^1 \frac{dz'}{z'} \frac{H_{i,k}(z', Q^2, m^2)}{z - z'} \\ &= \frac{1}{\pi} \sum_{n=1}^{\infty} z^{-n} \int\limits_0^1 dz' z'^{n-1} H_{i,g}(z', Q^2, m^2) \,. \end{aligned} \tag{57}$$

The graph for $T_{i,g}^{(1)}$ in Fig. 14 [1] yields the following integral

$$\begin{aligned} T_{i,g}^{(1)} &= g^2 P_i^{\mu\nu} \varepsilon^{\lambda}(p) \varepsilon^{\sigma}(p) \\ &\quad \times \int \frac{d^N k}{(2\pi)^N} \frac{\gamma_\lambda (\not{k} + m) \gamma_\mu (\not{k} + \not{q} + m) \gamma_\nu (\not{k} + m) \gamma_\sigma}{[(k-p)^2 - m^2](k^2 - m^2)^2 [(k+q)^2 - m^2]} \\ &\equiv \int d^N k \, f(k, q, p, m) \,. \end{aligned} \tag{58}$$

where $P_i^{\mu\nu}$ is a projection operator with $i = 2, L$ and $\varepsilon^{\lambda}(p)$ stands for the polarization vector of the gluon. In the limit $Q^2 \gg m^2$ the above expression will be called $T_{i,g}^{\mathrm{ASYMP},(1)}$ which can be split into the coefficient function

$$\begin{aligned} &\frac{1}{\pi} \sum_{n=1}^{\infty} z^{-n} \int\limits_0^1 dz' z'^{n-1} C_{i,g}^{(1)}\left(z', \frac{Q^2}{\mu^2}\right) \\ &= \left[\lim_{Q^2 \gg m^2} \int d^N k \, f(k, q, p, m) - \int d^N k \lim_{Q^2 \gg m^2} f(k, q, p, m) \right], \end{aligned} \tag{59}$$

[1] Notice that the lowest order Feynman graphs, shown in this section, are not complete. Current conservation and gauge invariance require additional graphs.

and the operator matrix element

$$\frac{1}{\pi}\sum_{n=1}^{\infty} z^{-n}\int_0^1 dz' z'^{n-1} A_{cg}^{(1)}\left(z', \frac{\mu^2}{m^2}\right) = \int d^N k \lim_{Q^2 \gg m^2} f(k,q,p,m)\,. \quad (60)$$

The first term in $T_{i,g}^{\mathrm{ASYMP},(1)}$ has no singularity at $m = 0$ and it carries the whole Q^2-dependence. The absence of the C-singularity can be checked by taking $k \propto p$. The dependence on m is transferred to $A_{cg}^{(1)}$ which however is independent of $q^2 = -Q^2$ as we will show below. Further by interchanging limits and integrations in Eqs. (59) and (60) one introduces an artificial UV singularity which has to be subtracted before one gets the finite $C_{i,g}^{(1)}$ and $A_{cg}^{(1)}$. To evaluate the expression in Eq. (60) we make the Taylor expansion

$$\frac{\gamma_\mu(\not{k}+\not{q}+m)\gamma_\nu}{(k+q)^2-m^2} = \frac{1}{q^2}\sum_{n=1}^{\infty} \gamma_\mu \not{q} \gamma_\nu \left(\frac{2k\cdot q}{-q^2}\right)^{n-1}$$
$$= -\sum_{n=1}^{\infty} \frac{2^{n-1}}{(-q^2)^n}\gamma_\mu\gamma_{\mu_1}\gamma_\nu k_{\mu_2}\cdots k_{\mu_n} q^{\mu_1}\cdots q^{\mu_n}\,, \quad (61)$$

so that we get

$$\frac{1}{\pi}\sum_{n=1}^{\infty} z^{-n}\int_0^1 dz' z'^{n-1} A_{cg}^{(1)}\left(z', \frac{\mu^2}{m^2}\right) = -g^2 \sum_{n=1}^{\infty} \frac{2^{n-1}}{(-q^2)^n} q^{\mu_1}\cdots q^{\mu_n}$$
$$\times P_i^{\mu\nu}\varepsilon^\lambda(p)\varepsilon^\sigma(p)\int \frac{d^N k}{(2\pi)^N} \frac{\gamma_\lambda(\not{k}+m)\gamma_\mu\gamma_{\mu_1}\gamma_\nu(\not{k}+m)\gamma_\sigma}{[(k-p)^2-m^2](k^2-m^2)^2} k_{\mu_2}\cdots k_{\mu_n}\,, \quad (62)$$

The vertex $2^{n-1}\gamma_{\mu_1} k_{\mu_2}\cdots k_{\mu_n}$ originates from the heavy quark operator matrix element (OME) given by

$$\langle c(k) \mid O_{c,\mu_1\cdots\mu_n}(0) \mid c(k)\rangle\,. \quad (63)$$

The heavy quark operator, which is a gauge invariant object (physical operator), is defined by

$$O_{c,\mu_1\cdots\mu_n}(x) = \bar{\psi}(x)\gamma_{\mu_1} D_{\mu_2}\cdots D_{\mu_n}\psi(x)\,, \quad (64)$$

with the heavy quark (charm) field ψ and the covariant derivative $D_\mu = \partial_\mu + igA_\mu$. If we now sandwich the above operator between physical gluon

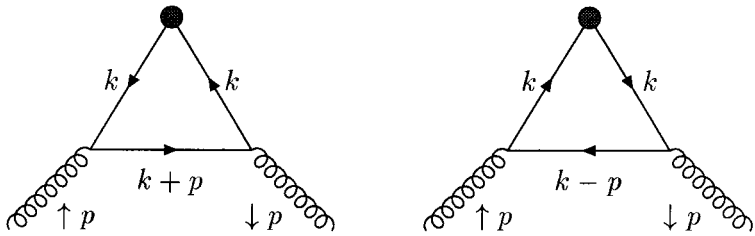

Fig. 15. Operator graphs corresponding with the operator matrix element $A_{cg}^{(1)}$.

states one obtains

$$\begin{aligned}
&\langle g(k) \mid O_{c,\mu_1\cdots\mu_n}(0) \mid g(k)\rangle \\
&= g^2\varepsilon^\lambda(p)\varepsilon^\sigma(p)\int \frac{d^Nk}{(2\pi)^N}\frac{\gamma_\lambda(\not k+m)\gamma_{\mu_1}(\not k+m)\gamma_\sigma}{[(k-p)^2-m^2](k^2-m^2)^2}k_{\mu_2}\cdots k_{\mu_n} \\
&= \hat{A}_{cg}^{(1),n}\left(\frac{\mu^2}{m^2}\right)[p_{\mu_1}\cdots p_{\mu_n} - g_{\mu_1\mu_2}p_{\mu_3}\cdots p_{\mu_n} \\
&\quad -g_{\mu_1\mu_2}g_{\mu_3\mu_4}p_{\mu_5}\cdots p_{\mu_n}\cdots]_{\text{symmetric}}\,. \qquad (65)
\end{aligned}$$

Notice that the projection which survives in Eq. (62) is given by $i = 2$ since $P_2^{\mu\nu}$ contains the metric tensor $g_{\mu\nu}$ only. Projections containing the vectors q^μ and p^μ vanish because of current conservation and the on-shell condition $p^2 = 0$ respectively. Therefore $T_{L,g}^{\text{ASYMP},(1)}$ and also $H_{L,g}^{\text{ASYMP},(1)}$ have no C-divergence for $m = 0$ and the only contribution comes from $\mathcal{C}_{L,g}^{(1)}$ which is Q^2 independent. The equality between Eq. (62) and Eq. (65) shows that the former represents the OME $A_{cg}^{(1)}$ as announced below Eq. (55). It is now easy to extract the OME if Eq. (65) is contracted by the tensor $\Delta_{\mu_1}\Delta_{\mu_2}\cdots\Delta_{\mu_n}$ where Δ_μ is a lightlike vector *i.e.* $\Delta^2 = 0$. Hence we get the expression

$$\hat{A}_{cg}^{(1),n}\left(\frac{\mu^2}{m^2}\right) = \int_0^1 dz' z'^{n-1} a_s\left[P_{qg}^{(0)}(z')\left(\frac{1}{\varepsilon_{UV}} + \frac{1}{2}\ln\left(\frac{\mu^2}{m^2}\right)\right) + a_{qg}^{(1)}(z')\right], \qquad (66)$$

with

$$A_{cg}^{(1)}\left(z, \frac{\mu^2}{m^2}\right) = \frac{1}{\pi}\sum_{n=1}^{\infty} z^{-n} A_{cg}^{(1),n}\left(\frac{\mu^2}{m^2}\right). \qquad (67)$$

After subtraction of the UV pole term, for which we choose the $\overline{\text{MS}}$-scheme, one obtains the finite OME in Eq. (54). The finite coefficient function $\mathcal{C}_{2,g}^{(1)}$ Eq. (53) is obtained from Eq. (59) in a similar way.

Generalizing mass factorization to higher orders one can write

$$H_{i,k}^{\text{ASYMP}}(Q^2, m^2) = A_{lk}\left(\frac{\mu^2}{m^2}\right) \otimes \mathcal{C}_{i,l}\left(\frac{Q^2}{\mu^2}\right). \qquad (68)$$

If we expand the OME's A_{kl} and the light parton coefficient functions $\mathcal{C}_{i,k}$ up to order α_s^2 one obtains the following equations

$$H_{i,g}^{\mathrm{ASYMP},(1)} = A_{cg}^{(1)} \otimes \mathcal{C}_{i,c}^{(0)} + A_{gg}^{(0)} \otimes \mathcal{C}_{i,g}^{(1)}, \tag{69}$$

$$H_{i,g}^{\mathrm{ASYMP},(2)} = A_{cg}^{(2)} \otimes \mathcal{C}_{i,c}^{(0)} + A_{cg}^{(1)} \otimes \mathcal{C}_{i,c}^{(1)} + A_{gg}^{(0)} \otimes \mathcal{C}_{i,g}^{(2)}, \tag{70}$$

$$H_{i,q}^{\mathrm{ASYMP},(2)} = A_{cq}^{(2)} \otimes \mathcal{C}_{i,c}^{(0)} + A_{qq}^{(0)} \otimes \mathcal{C}_{i,q}^{(2)}. \tag{71}$$

Here A_{gg} is obtained by sandwiching the gauge invariant gluonic operator

$$O_{g,\mu_1 \cdots \mu_n}(x) = F_{\mu_1}^{\alpha} D_{\mu_2} \cdots D_{\mu_{n-1}} F_{\mu_n,\alpha}, \tag{72}$$

between physical gluon states The heavy quark coefficient functions $L_{i,k}$ have to be added to $\mathcal{C}_{i,k}$ before we can apply mass factorization

$$\mathcal{C}_{i,k}\left(n_f, \frac{Q^2}{\mu^2}\right) + L_{i,k}^{\mathrm{ASYMP}}(Q^2, m^2) = A_{lk,c}\left(\frac{\mu^2}{m^2}\right) \otimes \mathcal{C}_{i,l}\left(n_f + 1, \frac{Q^2}{\mu^2}\right). \tag{73}$$

This relation also involves a redefinition of the strong coupling constant which in the right-hand-side now depends on $n_f + 1$ instead of n_f. The main effect of this operation is that the number of light flavours n_f appearing in $\mathcal{C}_{i,k}$ is enhanced by one unit. The $A_{kl,c}$ are given by all light parton OME's containing charm loop contributions to the gluon self energy only. Up to order α_s^2 we have

$$L_{i,k}^{\mathrm{ASYMP},(2)} = A_{qq,c}^{(2)} \otimes \mathcal{C}_{i,q}^{(0)} + A_{qq}^{(0)} \otimes \mathcal{C}_{i,q}^{(2)} + a_s \beta_{0,c} \mathcal{C}_{i,q}^{(1)} \ln\left(\frac{m^2}{\mu^2}\right). \tag{74}$$

Finally we want to emphasize that beyond the second order the above mass factorization relations become much more complicated. Here the heavy quark OME's A_{ck} can also contribute to Eq. (73) whereas the OME's $A_{kl,c}$ also enter Eq. (68). Using the mass factorization relations in Eqs. (69)-(71) we have computed the asymptotic heavy quark coefficient functions $H_{i,k}^{\mathrm{ASYMP},(2)}$ for $k = q, g$ and $i = 2, L$ in [15]. The same was done for $L_{i,q}^{\mathrm{ASYMP},(2)}$ Eq. (74). This was possible because the light parton coefficient functions and the heavy quark OME's were already known in [16] and [15] respectively. The expressions reveal the following characteristic behaviour

$$H_{i,k}^{\mathrm{ASYMP},(l)}(z, Q^2, m^2, \mu^2) \sim \alpha_s^l \sum_{n+j \leq l} a_{nj}(z) \ln^n\left(\frac{\mu^2}{m^2}\right) \ln^j\left(\frac{Q^2}{m^2}\right), \tag{75}$$

with an analogous expression for $L_{i,k}^{\mathrm{ASYMP}}$. One of the most important features, discovered in [15], is that the asymptotic expressions tend to the exact

heavy quark coefficient functions at rather low ξ-values (see Eq. (43)) provided z is not too small. According to Ref. [15] $\xi = 10$ for $z < 0.01$ which in charm production corresponds to $Q^2 = 22.5\,(\mathrm{GeV}/c)^2$ with $m = 1.5\ \mathrm{GeV}/c$ The consequences of this behaviour for the charm component of the structure function will be discussed in the next section.

5. Description of $F_{i,c}$ in the various schemes

In the literature one has proposed various descriptions of the charm component of the structure function in the framework of extrinsic charm production. Here one can distinguish the following schemes.

1 The three flavour number scheme (TFNS)

Here the production mechanisms are given by the photon-gluon fusion process and the higher order reactions. The charm component of the structure function $F_{i,c}$ is given by Eq. (37). The parton densities are given by the three light flavour densities u, d, s and the gluon density g.

2 The four flavour number scheme (FFNS)

In this case $F_{i,c}$ is expressed into convolutions of light parton coefficient functions with light parton densities. The latter are represented by four light flavours, which includes the charm quark, and the gluon.

3 The variable-flavour number scheme (VFNS)

This scheme interpolates between the results of the structure functions $F_{i,c}$ obtained from the TFNS and the FFNS.

In this section we will now derive the expressions for $F_{i,c}$ in the FFNS and the VFNS from the TFNS .

In order to derive $F_{i,c}^{\mathrm{FFNS}}$ we need the deep inelastic structure function which receives contributions from subprocesses containing light partons in the initial and final state only. It is given by

$$\begin{aligned} & F_i(n_f, Q^2) \\ &= \frac{1}{n_f} \sum_{k=1}^{n_f} e_k^2 \left[f_q^{\mathrm{S}}(n_f, \mu^2) \otimes C_{i,q}^{\mathrm{S}}\left(n_f, \frac{Q^2}{\mu^2}\right) + f_g^{\mathrm{S}}(n_f, \mu^2) \otimes C_{i,g}^{\mathrm{S}}\left(n_f, \frac{Q^2}{\mu^2}\right) \right. \\ & \left. + n_f f_k^{\mathrm{NS}}(n_f, \mu^2) \otimes C_{i,q}^{\mathrm{NS}}\left(n_f, \frac{Q^2}{\mu^2}\right) \right]. \end{aligned} \tag{76}$$

In the case of TFNS we have to choose $n_f = 3$. In the above expression the coefficient functions $C_{i,k}$ contain heavy quark loop contributions to the

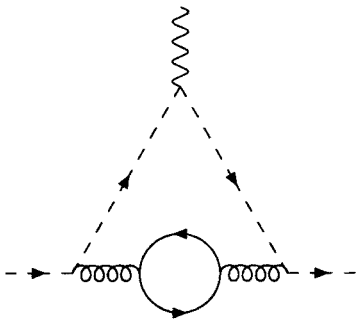

Fig. 16. Two-loop vertex correction containing a heavy quark loop. It contributes to $C_{i,q}$.

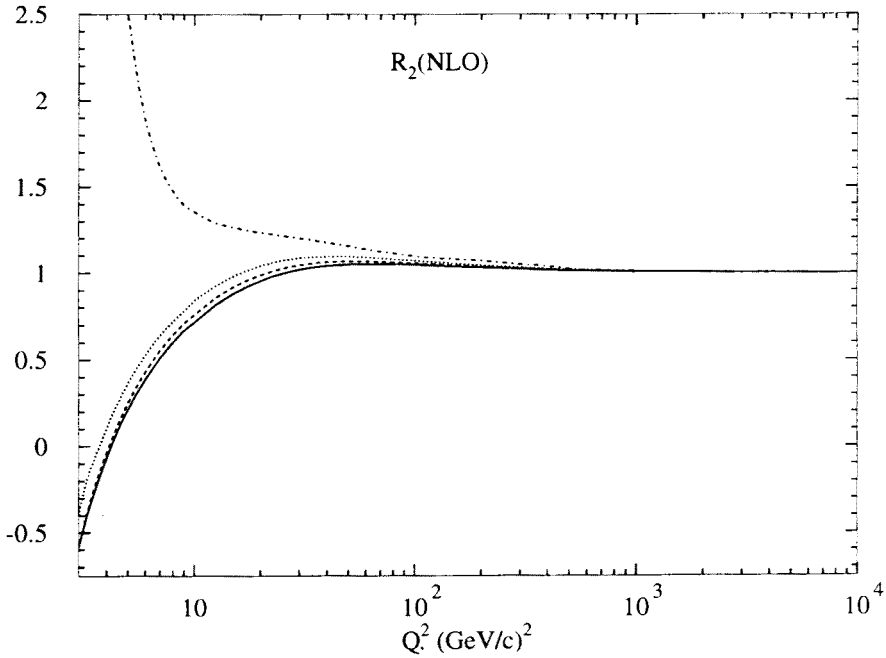

Fig. 17. R_2(NLO) plotted as a function of Q^2 at fixed x; $x = 0.1$ (dashed-dotted line), $x = 0.01$ (dotted line), $x = 10^{-3}$ (dashed line) , $x = 10^{-4}$ (solid line).

gluon self energies appearing in the light partonic matrix elements. This happens for the first time in order α_s^2. An example is shown in Fig. 16. The charm quark loop contributions will now be removed from $F_i(n_f, Q^2)$ and added to $F_{i,c}$ in (37). In the subsequent part of this section the latter

will be called $F_{i,c}^{\mathrm{EXACT}}$. In this way the coefficient functions $L_{i,k}$ get the proper asymptotic behaviour when $Q^2 \gg m^2$ as indicated in Eq. (75). This allows us to perform mass factorization after we have added the light parton coefficient function $\mathcal{C}_{i,k}$ in which all contributions from heavy quark loops are removed (see Eq. (73)). Next we define the following quantity

$$F_{i,c}^{\mathrm{ASYMP}}(n_f, x, Q^2, m^2) = \lim_{Q^2 \gg m^2} \left[F_{i,c}^{\mathrm{EXACT}}(n_f, x, Q^2, m^2) \right]. \tag{77}$$

Notice that $F_{i,c}^{\mathrm{ASYMP}}$ is given by the same expression as $F_{i,c}^{\mathrm{EXACT}}$ except that now the exact heavy quark coefficient functions are replaced by their asymptotic analogues which have the form presented in Eq. (75). In Fig. 17 we have plotted in next-to-leading order (NLO) the ratio

$$R_2(x, Q^2, m_c^2) = \frac{F_{2,c}^{\mathrm{ASYMP}}(x, Q^2, m_c^2)}{F_{2,c}^{\mathrm{EXACT}}(x, Q^2, m_c^2)}. \tag{78}$$

For this plot we have adopted the parton density set with $\Lambda_4 = 200$ MeV from [18] ($\overline{\mathrm{MS}}$-scheme). The mass factorization scale is chosen to be $\mu = Q$. The charm quark mass is equal to $m_c = 1.5\ \mathrm{GeV}/c$. From this figure we infer that for $Q^2 > 20\ (\mathrm{GeV}/c)^2$ and $x < 0.01$, $F_{2,c}^{\mathrm{ASYMP}}$ coincides with $F_{2,c}^{\mathrm{EXACT}}$. For $F_{L,c}$ this happens when Q^2 is much larger *i.e.* $Q^2 > 1000\ (\mathrm{GeV}/c)^2$. This implies that the large logarithmic terms in the heavy quark coefficient functions $H_{i,k}$ and $L_{i,k}$ as given by Eq. (75) entirely determine the charm component of the structure function. Since these corrections vitiate the perturbation series when Q^2 gets large they should be resummed in all orders of perturbation theory. This procedure has been carried out in [17] and it consists of four steps. First we add $F_i(n_f, Q^2)$ in Eq. (76) to $F_{i,c}^{\mathrm{ASYMP}}(n_f, x, Q^2, m^2)$ in Eq. (77) and choose $n_f = 3$. Second we apply mass factorization to the asymptotic heavy quark coefficient functions according to Eqs. (68), (73). In the third step we define new parton densities which are now presented in a four flavour number scheme (FFNS). For the three light flavour densities $k = u, d, s$ we have

$$\begin{aligned} f_k(4,\mu^2) + f_{\bar{k}}(4,\mu^2) = {} & A_{qq,c}^{\mathrm{NS}}\left(3, \frac{\mu^2}{m^2}\right) \otimes \left[f_k(3,\mu^2) + f_{\bar{k}}(3,\mu^2) \right] \\ & + \tilde{A}_{qq,c}^{\mathrm{PS}}\left(3, \frac{\mu^2}{m^2}\right) \otimes \Sigma(3,\mu^2) \\ & + \tilde{A}_{qg,c}^{\mathrm{S}}\left(3, \frac{\mu^2}{m^2}\right) \otimes G(3,\mu^2). \end{aligned} \tag{79}$$

The gluon density in the FFNS reads

$$G(4,\mu^2) = A_{gq,c}^{\mathrm{S}}(3,\mu^2) \otimes \Sigma(3,\mu^2) + A_{gg,c}^{\mathrm{S}}(3,\mu^2) \otimes G(3,\mu^2). \tag{80}$$

Finally we get a new light flavour density represented by the charm quark

$$f_{c+\bar{c}}(4,\mu^2) \equiv f_4(4,\mu^2) + f_{\bar{4}}(4,\mu^2)$$
$$= A_{cq}^{\mathrm{S}}\left(3,\frac{\mu^2}{m^2}\right) \otimes \Sigma(3,\mu^2) + A_{cg}^{\mathrm{S}}\left(3,\frac{\mu^2}{m^2}\right) \otimes G(3,\mu^2)\,. \quad (81)$$

The above charm quark density has the property that it does not vanish at $\mu = m$ in the $\overline{\mathrm{MS}}$-scheme contrary to what is usually assumed in the literature (see *e.g.* [19–22]. In the fourth step we rearrange terms and obtain

$$F_{i,c}^{\mathrm{ASYMP}}(n_f,x,Q^2,m^2) + F_i(n_f,x,Q^2) = F_i(n_f+1,x,Q^2)\,, \quad (82)$$

which is the FFNS result for the total structure function. From the latter quantity one can extract the expression for the charm quark component of the proton structure function in the FFNS which will be denoted by

$$F_{i,c}^{\mathrm{PDF}}(n_f+1,Q^2)$$
$$= e_c^2\left[f_{c+\bar{c}}(n_f+1,\mu^2) \otimes C_{i,q}^{\mathrm{NS}}\left(n_f+1,\frac{Q^2}{\mu^2}\right) + \Sigma(n_f+1,\mu^2)\right.$$
$$\left. \otimes \tilde{C}_{i,q}^{\mathrm{PS}}\left(n_f+1,\frac{Q^2}{\mu^2}\right) + G(n_f+1,\mu^2) \otimes \tilde{C}_{i,g}^{\mathrm{S}}\left(n_f+1,\frac{Q^2}{\mu^2}\right)\right], \quad (83)$$

where we have defined

$$C_{i,q}^{\mathrm{S}}(n_f) = C_{i,q}^{\mathrm{NS}}(n_f) + n_f \tilde{C}_{i,q}^{\mathrm{PS}}(n_f)\,, \qquad C_{i,g}^{\mathrm{S}} = n_f \tilde{C}_{i,g}^{\mathrm{S}}\,. \quad (84)$$

The superscript PDF in Eq. (83) stands for parton density function which means that the charm component of the structure function is completely expressed into parton densities multiplied by the light parton coefficient functions. Notice that $F_{i,c}^{\mathrm{PDF}}$ is a renormalization group invariant like $F_{i,c}^{\mathrm{EXACT}}$ and $F_{i,c}^{\mathrm{ASYMP}}$ so that they satisfy the equation $D\,F_{i,c} = 0$ (see Eq. (38) and below). Further $F_{i,c}^{\mathrm{PDF}}$ originates from the charm quark coefficient functions $H_{i,k}$ from which it follows that the former is proportional to e_c^2 only. The functions $L_{i,k}$, which are multiplied by the light charge squared e_k^2, contribute to both $F_{i,c}^{\mathrm{PDF}}(n_f+1,Q^2)$ and $F_2(n_f+1,Q^2)$ so that the number of flavours in these structure functions are increased by one unit. The FFNS charm quark density is mainly determined by the size of the TFNS gluon density $G(n_f,z,\mu^2)$ for $n_f = 3$. Therefore the latter plays a major role in the behaviour of $F_{i,c}^{\mathrm{EXACT}}$ as well as of $F_{i,c}^{\mathrm{PDF}}$. An analysis of both structure functions in [17] reveals that the former gives the best description of charm production in the threshold region where Q^2 is small and x is large. On the other hand when Q^2 is large and x is small it turns out that it is better to

use $F_{2,c}^{\rm PDF}$ because it is in this region where the large logarithms in Eq. (75) dominate so that they have to be resummed. Therefore the TFNS is the most suitable scheme for the charm component of the structure function near threshold whereas far away from this region it turns out that the FFNS is more appropriate.

One also needs a scheme which merges the advantages of these two pictures and provides us with good description of $F_{2,c}$ in the intermediate regime in Q^2. This is given by the so called variable flavour number scheme (VFNS). In [17] we proposed the following VFNS structure function

$$F_{i,c}^{\rm VFNS}(x,Q^2,m^2) = F_{i,c}^{\rm PDF}(n_f+1,x,Q^2) + F_{i,c}^{\rm EXACT}(n_f,x,Q^2,m^2) - F_{i,c}^{\rm ASYMP}(n_f,x,Q^2,m^2)\,. \tag{85}$$

The above expression is a generalization of Eq. (9) in [23], which was only presented in leading order (LO) and has been implemented in a recent global parton density analysis [22]. (A different VFNS scheme has recently been proposed in [24].) In LO the VFNS scheme has the properties that for $Q^2 \gg m^2$, $F_{2,c}^{\rm EXACT} \to F_{2,c}^{\rm ASYMP}$ which means that $F_{2,c}^{\rm VFNS} \to F_{2,c}^{\rm PDF}$. Further at low Q^2 (*i.e.* $Q^2 \leq m^2$) $F_{2,c}^{\rm ASYMP} \to F_{2,c}^{\rm PDF}$ so that $F_{2,c}^{\rm VFNS} \to F_{2,c}^{\rm EXACT}$. provided we put $z_{\max} = 1$ in $F_{2,c}^{\rm ASYMP}$. However the last relation is no longer true in higher order in α_s. The main reason is that new production mechanisms appear in NLO giving rise to the coefficient functions $L_{i,k}$. The latter contain the prefactor e_k^2 (*e.g.* the Compton process) and show up in $F_{2,c}^{\rm EXACT}$ and $F_{2,c}^{\rm ASYMP}$ but not in $F_{2,c}^{\rm PDF}$, which is proportional to e_c^2 only (see Eq. (83)). This higher order effect is only noticeable in the threshold regime where x is very large and Q^2 is very small.

As an application we have studied the charm component of the proton structure function in the three schemes mentioned above. The coefficient functions used for these structure functions are all computed up to order α_s^2 (see [2, 15, 16]) so that we will denote them by $F_{2,c}^{\rm EXACT,(2)}$ (Eq. (37)), $F_{2,c}^{\rm PDF,(2)}$ (Eq. (83)) and $F_{2,c}^{\rm VFNS,(2)}$ (Eq. (85)). In Fig. 18 we have plotted the scale (μ) dependence up to NLO of the structure functions in the different schemes mentioned above. For these plots we used the parton densities presented in the $\overline{\rm MS}$-scheme with $\Lambda_4 = 200$ MeV in [20]. The scale μ is adopted from [23] and it is given by

$$\begin{aligned} \mu^2 &= m^2 + kQ^2(1-m^2/Q^2)^n \quad \text{for} \quad Q^2 > m^2\,, \\ &= m^2 \quad \text{for} \quad Q^2 \leq m^2\,, \end{aligned} \tag{86}$$

with $k = 0.5$, $n = 2$ and $m = 1.5$ (GeV/c^2). In [23] and in [25] it was shown that $F_{2,c}^{\rm VFNS}$ in LO is less sensitive to variations in the scale μ than each term on the right-hand-side of Eq. (85) separately. However in NLO

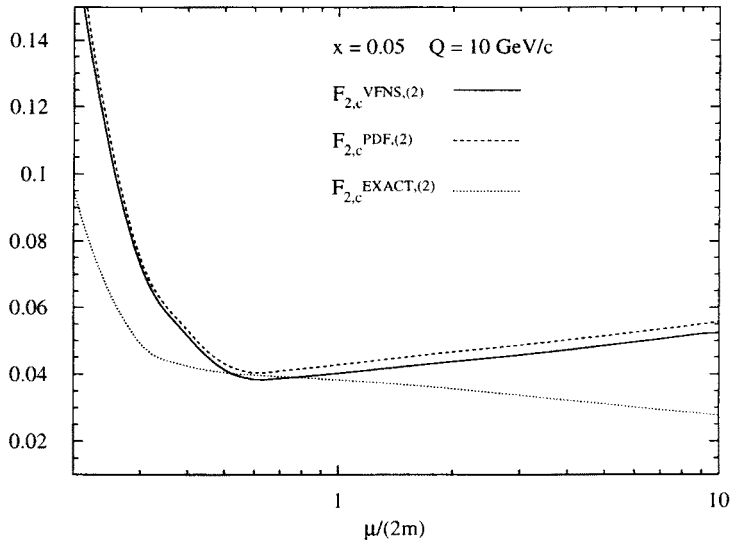

Fig. 18. Scale dependence of the structure functions at $x = 0.05$ and $Q = 10$ GeV/c; $F_{2,c}^{\mathrm{VFNS},(2)}$ (solid line), $F_{2,c}^{\mathrm{PDF},(2)}$ (dashed line), $F_{2,c}^{\mathrm{EXACT},(2)}$ (dotted line).

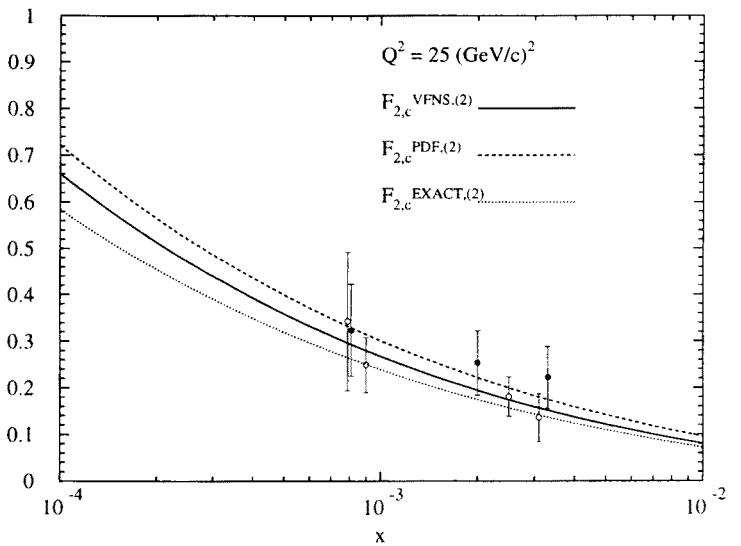

Fig. 19. Structure functions at $Q^2 = 25$ (GeV/c)^2; $F_{2,c}^{\mathrm{VFNS},(2)}$ (solid line), $F_{2,c}^{\mathrm{PDF},(2)}$ (dashed line), $F_{2,c}^{\mathrm{EXACT},(2)}$ (dotted line). The experimental data are from [6] (closed circles) and [7] (open circles).

we observe in Fig. 18 that there is no reason to prefer one scheme over the other. This is corroborated by the findings in [26] and [12] where one could show that there is a considerable improvement in $F_{2,c}^{\mathrm{EXACT},(2)}$ with respect to variations in the mass factorization scale when this quantity is computed up to NLO. In Fig. 19 we plot $F_{2,c}$ in the three different schemes and compare the results with the recent data from the H1 [6] and ZEUS [7] collaborations. Further we have chosen the parton density set in [19] with $\Lambda_4 = 200$ MeV. Notice that all parton density sets in [22, 20, 19] used for the plots of the structure functions are presented in FFNS although in principle one has to choose a TFNS parametrization for both the parton densities (see *e.g.* [18]) and the running coupling constant for the computation of $F_{2,c}^{\mathrm{EXACT}}$

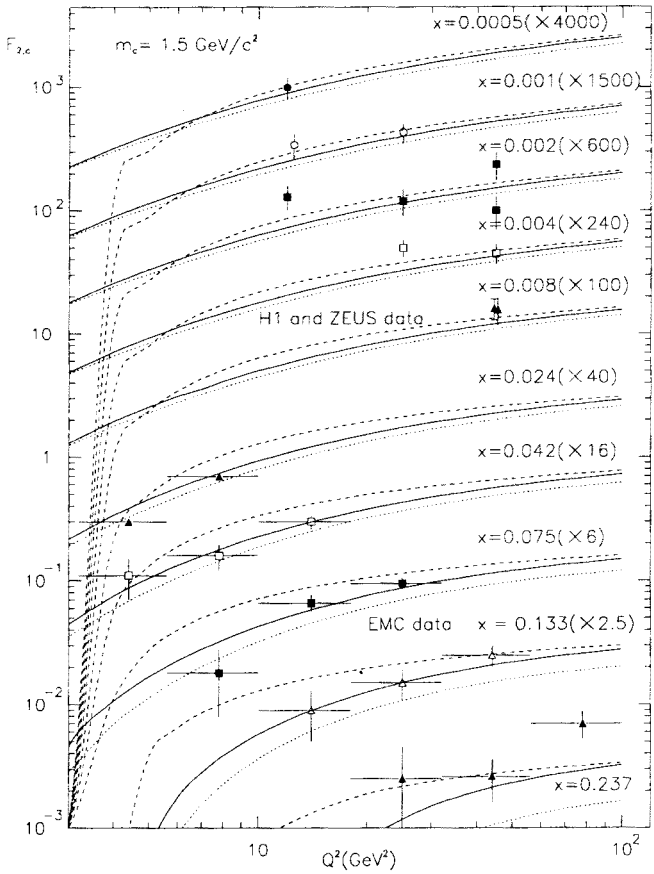

Fig. 20. Structure functions $F_{2,c}^{\mathrm{VFNS},(2)}$ (solid line), $F_{2,c}^{\mathrm{PDF},(2)}$ (dashed line), $F_{2,c}^{\mathrm{EXACT},(2)}$ (dotted line). The experimental data are from [27, 6] and [7].

and $F_{2,c}^{\mathrm{ASYMP}}$. However we have checked that the latter are not significantly altered when we replace the parton densities in [18] by those in [19]. From Fig. 19 we infer that the data are in agreement with all schemes in which the structure functions are computed. Further the results for $F_{2,c}^{\mathrm{VFNS},(2)}$ are always between $F_{2,c}^{\mathrm{EXACT},(2)}$ and $F_{2,c}^{\mathrm{PDF},(2)}$. It is clear that one needs more precise data in finer bins of x and Q^2 to discriminate between the various schemes. Finally we have made a comparison with the data in the small x-region as well as in the large x-region obtained by the experimental groups H1 [6], ZEUS [7] and EMC [27] respectively. The plots for the various schemes are shown in Fig. 20. The agreement between the data and the predictions from the structure functions in Eq. (85) is fairly good except for $x = 0.237$. The discrepancy occuring in the threshold region is mainly due to the large negative contribution coming from Fig. 16 and the chosen scale in Eq. (86) which originates from [23]. It turns out that at low Q^2 this scale becomes too small so that the running coupling constant is too big. In this region all schemes lead to negative structure functions in particular for $F_{2,c}^{\mathrm{EXACT}}$. Therefore perturbation theory breaks down and one has to choose a larger scale. This phenomenon, which was not observed in the LO analysis in [23], only appears when the NLO corrections are taken into account.

We would like to thank J. Smith and Y. Matiounine for the careful reading of the manuscript and for giving us some useful comments.

References

[1] A. Ali, *Acta. Phys. Pol.* **B27**, 3529 (1996).

[2] E. Laenen, S. Riemersma, J. Smith, W.L. van Neerven, *Nucl. Phys.* **B392**, 162 (1993).

[3] E. Laenen, S. Riemersma, J. Smith, W.L. van Neerven, *Nucl. Phys.* **B392**, 229 (1993) 229; B.W. Harris, J. Smith, *Nucl. Phys.* **B452** (1995) 109.

[4] S.J. Brodsky, P. Hoyer, A.H. Mueller, W.-K. Tang, *Nucl. Phys.* **B369**, 519 (1992); R. Vogt, S.J. Brodsky, *Nucl. Phys.* **B438**, 261 (1995).

[5] E. Witten, *Nucl. Phys.* **B104**, 445 (1976); J. Babcock, D. Sivers, *Phys. Rev.* **D18**, 2301 (1978); M.A. Shifman, A.I. Vainstein, V.J. Zakharov, *Nucl. Phys.* **B136**, 157 (1978); M. Glück, E. Reya, *Phys. Lett.* **B83**, 98 (1979); J.V. Leveille, T. Weiler, *Nucl. Phys.* **B147**, 147 (1979).

[6] H1 Collaboration, C. Adloff *et al.*, *Z. Phys.* **C72**, 593 (1996).

[7] ZEUS Collaboration, M. Derrick *et al.*, *Phys. Lett.* **B349** 225 (1995); ZEUS Collaboration, M. Derrick *et al.*, XXVII Int. Conf. on HEP '96, Warsaw (1996); ZEUS Collaboration, J. Breitweg *et al.*, DESY-97-089.

[8] F. Bloch, A. Nordsieck, *Phys. Rev.* **52**, 54 (1937).

[9] T. Kinoshita, *J. Math. Phys.* **3**, 650 (1962); T.D.Lee, M. Nauenberg, *Phys. Rev.* **133**, B1549 (1964).

[10] V.N. Gribov, L.N. Lipatov, *Sov. J. Nucl. Phys.* **15**, 438, 675 (1972); G. Altarelli, G. Parisi, *Nucl. Phys.* **B126**, 298 (1977); Yu. Dokshitser, *Sov. Phys. JETP* **46**, 641 (1977).

[11] S. Riemersma, J. Smith, W.L. van Neerven, *Phys. Lett.* **B347**, 143 (1995).

[12] A. Vogt, DESY 96-012, hep-ph/9601352;

[13] E. Laenen, J. Smith, W.L. van Neerven, *Nucl. Phys.* **B369**, 543 (1992).

[14] S. Catani, M. Ciafaloni, F. Hautmann, *Phys. Lett.* **B242**, 97 (1990); Production of heavy flavours at high energies, Proc. Workshop "Physics at HERA, Hamburg, Oct. 29-30, 1991, eds. W. Buchmüller and G. Ingelman, Vol. 2, p. 690.

[15] M. Buza, Y. Matiounine, J. Smith, R. Migneron, W.L. van Neerven, *Nucl. Phys.* **B472**, 611 (1996).

[16] E.B. Zijlstra, W.L. van Neerven, *Nucl. Phys.* **B383**, 525 (1992).

[17] M. Buza, Y. Matiounine, J. Smith, and W.L. van Neerven, DESY 96-278, hep-ph/9612398, to be published in *Z. Phys.* **C** (1997).

[18] M. Glück, E. Reya, A. Vogt, *Z. Phys.* **C67**, 433 (1995).

[19] M. Glück, E. Reya, A. Vogt, *Z. Phys.* **C53**, 127 (1992).

[20] H.L. Lai *et al.* (CTEQ-collaboration), *Phys. Rev.* **D51**, 4763 (1995).

[21] A.D. Martin, R.G. Roberts, W.J. Stirling, *Phys. Lett.* **B387**, 419 (1996).

[22] H.L. Lai, W.K. Tung, *Z. Phys.* **C74**, 463 (1997).

[23] M.A.G. Aivazis, J.C. Collins, F.I. Olness, W.K. Tung, *Phys. Rev.* **D50**, 3102 (1994).

[24] A.D. Martin, R.G. Roberts, M.G. Ryskin, W.J. Stirling, DTP/96/102, RAL-TR-96-103, hep-ph/9612449.

[25] F.I. Olness, S. Riemersma, *Phys. Rev.* **D51**, 4746 (1995);

[26] M. Glück, E. Reya, M. Stratmann, *Nucl. Phys.* **B222**, 37 (1994).

[27] J.J. Aubert *et al.* (EMC Collab.), *Nucl. Phys.* **B213**, 31 (1983); see also B.W. Harris, J. Smith, R. Vogt, *Nucl. Phys.* **B461**, 181 (1996).